ISSN 1392–1320 MATERIALS SCIENCE (MEDŽIAGOTYRA). Vol. 16, No. 1. 2010

Deposition of Alumina Coatings from Nanopowders by Plasma Spraying

Liutauras MARCINAUSKAS*

Department of Physics, Kaunas University of Technology, Studentų 50, LT-51368 Kaunas, Lithuania
Lithuanian Energy Institute, Plasma Processing Laboratory, Breslaujos 3, LT-44403 Kaunas, Lithuania

Received 23 April 2009; accepted 31 August 2009

Aluminum oxide coatings were prepared by the atmospheric plasma spraying from the Al_2O_3 nanopowders. The powders were injected into the anode zone at high temperature region. Scanning electron microscopy (SEM) and X-ray diffraction (XRD) were applied to analyze the granulated nanopowder feedstocks and coatings. The results demonstrated that the higher the plasma torch power was the lower surface roughness. The XRD results showed that δ-Al_2O_3 was the main phase for granules dried for 12 h at 473 K. Meanwhile the as-sprayed coatings are composed of γ-Al_2O_3 and α-Al_2O_3. The increase of the plasma torch power leads to the production of the alumina coatings with a higher amount of the γ-Al_2O_3 phase. The crystallite size of γ-Al_2O_3 (400) phase decreases from 97 nm down to 49 nm with the increase of the torch power.
Keywords: Al_2O_3, plasma spraying, nanopowders.

INTRODUCTION

Nowadays γ-Al_2O_3 has been receiving considerable attention owing to its high elastic modulus, hardness, radiation resistance, thermal and chemical stability, and especially to its potential for broad applications in adsorbents, catalyst, catalyst supports, and advanced ceramics [1 – 6]. It was reported that CO can be effectively decomposed in γ-Al_2O_3 doped with a Cr_2O_3 and CuO catalyst [5]. Young [2] developed a new method to obtain alumina coatings with a significantly higher dielectric strength values. The γ-Al_2O_3 is used to support of Ni catalyst in hydrogen production by steam reforming of liquefied natural gas [3]. Therefore such a wide potential of application of the gamma alumina promotes to search a new methods and improve already existing for the production of γ-Al_2O_3 structures.

An atmospheric plasma spraying (APS) is one of the most popular methods for the production of alumina coatings. The main advantages of the APS technology are possibility to achieve a high temperatures (usually up to 15000 K) and high velocities (between 100 m/s and 2500 m/s) of plasma flow. When the ceramic powders (Al_2O_3, TiO_2, ZrO_2) are introduced in the plasma stream, they are immediately melted and accelerated to spray a coating [5 – 11]. Generally, because of the process nature, the structure of a sprayed coating is characterized by the lamellar structures with the existence of the microdefects (pores, splat boundaries, microcracks, and some unmelted particles) [11].

Recently, the scientific community has focused remarkable attention on the synthesis of ceramic coatings from the nanopowders. It has been demonstrated that the nanostructured plasma sprayed ceramic oxide (Al_2O_3, TiO_2, ZrO_2) coatings have higher hardness, wear resistance values, lower porosity values when compared to the similar coatings formed from the conventional powders [12 – 17]. It is well known that the physical, mechanical, tribological properties of the plasma sprayed coatings are dependent upon the processing parameters selected during spraying. The most important are plasma torch construction, substrate temperature, input power, plasma carried gas type, injection place of the particles, size of the particle, pressure, velocity and temperature of the plasma jet flow, etc [12 – 16]. The input power is an important parameter that affects the quality of the coating, since it changes the velocity and temperature of the particles at the moment of impinging the substrate. For instance, experimental research by Gao et al. [10] showed that the velocity of the powder particles increased with increasing the spraying power. It was showed that the Al_2O_3 coatings produced at a higher voltage and arc current values are denser and harder [8].

However, during the production of ceramic coatings from the nanopowders, beside early mentioned parameters new problems appear. The first one is feeding of the nanopowders in to the plasma. The nanopowders adhere to the walls of feeding system and are very difficult to arrive at the plasma torch due to its high specific area and low mass. To overcome this problem, reconstitution of the nanoparticles into micrometer sized granules is necessary. The majority of authors demonstrated that the most favorable size of these granules is in the range of 10 μm – 100 μm [12 – 16]. Other authors proposed to use a liquid feedstock carrier [17 – 20]. The nanopowders are dissolved in to the liquid and produced suspension is injected directly in to the plasma flame. The second challenge is to select the required process parameters, which will retain grain size at the nanometer regime in the deposited coatings [12, 17]. However, the systematic research on the effect of the plasma torch power on the Al_2O_3 properties of the coatings deposited from nanopowders was relatively few.

This paper presents a study on the formation of alumina coatings from the nanopowders using the plasma spraying technology. The purpose was to find out the effect of plasma torch power on the surface microstructure, phase composition, and γ-Al_2O_3 content of the alumina coatings.

*Corresponding author. Tel.: +370-611-17031; fax: +370-37-456472.
E-mail address: *liutauras@.mail.lei.lt* (L. Marcinauskas)

EXPERIMENTAL

The direct current plasma torch used in the experiments was developed by Lithuanian Energy Institute scientists. It consists of the copper cathode with the hafnium emitter, the working gas injecting ring with two tangential blowholes, and a step formed anode nozzle with blowhole. Both electrodes are cooled by water in order to prevent them from the erosion caused by enormous heat flux from the arc. The tangential plasma forming gas injection helps to stabilize the plasma arc flow. More details about the plasma torch can be found elsewhere [21]. Nitrogen was used as plasma forming gas (0.208 g/s), while argon (0.033 g/s) as Al_2O_3 powder carrier gas. The powders were introduced into the anode nozzle due to improve the melting efficiency of spray particles. It will lead to an increase of the dwell time of the granules in the hottest zone of the plasma jet. The coatings were formed on the stainless steel substrates at atmospheric pressure at a various plasma torch powers. The plasma torch – substrate distance was kept at 0.035 m, the spray duration was 180 s. Process parameters of the coatings are presented in Table 1.

Table 1. Preparation conditions of the alumina coatings

Current, A	43.2	52.0	64.6
Voltage, V	74	72	70
Torch power, kW	3.2	3.75	4.52

Ultra dispersion powder aluminium oxide (Sepros Corp. Int.) extracted by gas dispersion synthesis method was used as starting material. The average size of the alumina nanoparticles was – 87 nm, true density – 3610 kg/m^3, bulk density – 1890 kg/m^3, melting temperature – 2320 K. The composition of nanoparticles were aluminum oxide (Al_2O_3) – 99.950 %, magnesium oxide (MgO) – 0.011 %, silicon oxide (SiO_2) – 0.007 %, iron oxide (Fe_2O_3) – 0.002 %, titanium oxide (TiO_2) – 0.001 %, calcium oxide (CaO) – 0.017 %, sodium oxide (Na_2O) – 0.009 %. In order to make these nanosize powders sprayable, they were granulated into the various micro size particles and dried for 12 hours at 473 K (Fig. 1). The dried granules were sifted using a separator in order to select granules with the diameter less than 50 μm.

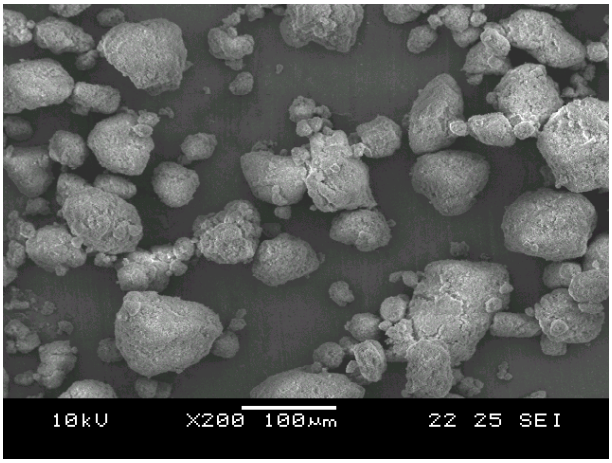

Fig. 1. SEM view of granulated Al_2O_3 powders

The surface morphology was characterized by scanning electron microscopy (SEM) model JEOL JSM-5600. The X-ray diffraction (XRD) measurements were carried out in a $10° - 70°$ range with CuK_α radiation ($\lambda = 0.15405$ nm) on a DRON diffractometer operating at 35 kV and 20 mA equipped with a single-crystal graphite monochromator in step scanning mode of 0.02° in 2θ and counting time of 0.5 s per step. The average crystallite size was calculated for the highest intensity gamma (400) and alpha (113) alumina diffraction peaks by using Scherrer's equation:

$$D = \frac{0.9\lambda}{\beta \cos\theta}, \quad (1)$$

where D is the crystallite size, λ is the wavelength of the X-rays, β is the full-width at half maximum (FWHM) of the corresponding line, and θ is the scattering angle of diffraction of the peak.

RESULTS AND DISCUSSIONS

SEM image of alumina granules before processing is shown in Fig. 1. It is clearly seen that the granules are in different irregular shapes, ranking from 5 μm to 100 μm. The deposited coatings are composed of various micro and nanosize particles. The particles are seen to be nearly spherical in shape, with the sizes in the range of 1 μm÷10 μm. It may be noted that beside micrometer size, there are many nanosize (100 nm – 500 nm) fragments (Fig. 2, b and d). The coating produced at the lowest torch power consists of a relatively higher amount of larger (>5 μm) dimension particles compared to the film produced at 4.52 kW. However the surfaces of these particles are covered by nanosize fragments (Fig. 2, b). Meanwhile, the surface of film deposited at 4.52 kW is covered by 1 μm – 2 μm particles and agglomerated nanoparticles clusters. Thus, the coatings are formed by fully or partially melted granules. The formation of the deposits includes the following processes: the granules are heated to fully or partially melting and accelerated in plasma jet, then strike into substrate, deforms and finally solidify to form the aluminum oxide coating. SEM pictures (Fig. 2) indicate clear boundaries between different sprayed granules. The existing lamination structure indicates that the layers are mainly mechanically adhered. The SEM results indicated that the surface roughness decreases with the increase of the torch power.

The XRD patterns of the feedstock granules and coatings at different powers are shown in Fig. 3. The results indicate that the alumina powders are nearly all δ-Al_2O_3 with minor amount of γ-Al_2O_3. The XRD diffraction patterns of the formed aluminum oxide coatings at different torch powers show that the positions of the Bragg peaks are typical for the cubic γ-Al_2O_3 and rhombohedral α-Al_2O_3 (Fig. 3). The dominant gamma phase peaks are attributed to (400) and (440) orientation. Meanwhile, the sharp α-Al_2O_3 (012), (104), (113), and (024) diffraction peaks are found in the coating obtained at 3.2 kW. The increase of the torch power leads to higher intensity of the γ-Al_2O_3 phase peaks. It may be noted that the coatings sprayed at the highest plasma torch power consist only from the cubic γ-Al_2O_3 phase (Fig. 3).

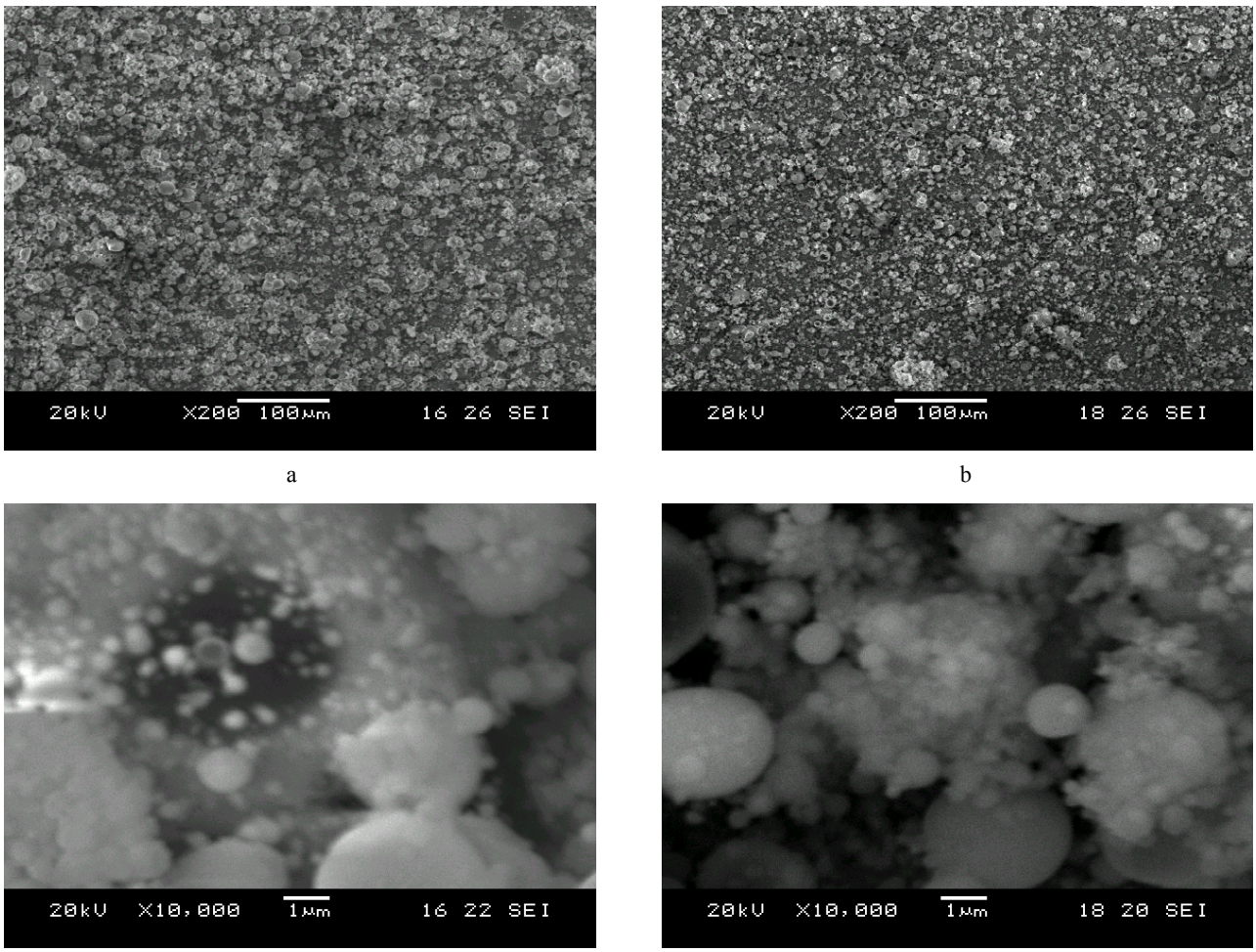

a b

c d

Fig. 2. SEM views of Al_2O_3 coatings formed at various plasma torch powers (a, b) 3.2 kW and (c, d) 4.52 kW

It has been demonstrated that the (γ-Al_2O_3 / / (α-Al_2O_3 + γ-Al_2O_3)) ratio can be effectively used as an indicator for optimal processing [22]. The relative amount of the major phases was calculated from the XRD intensity data [22, 23]:

$$R = \frac{I_{(400)}^{\gamma-Al_2O_3}}{I_{(113)}^{\alpha-Al_2O_3} + I_{(400)}^{\gamma-Al_2O_3}} \times 100\% \ , \qquad (2)$$

where $I_{(hkl)}$ is the intensity of the peak diffraction for the corresponding plane of the α-Al_2O_3, and γ-Al_2O_3 phases.

It was obtained that the γ-Al_2O_3 phase content (R) in the coatings is 56.52 %, 72.05 %, and 100 % for plasma torch powers 3.2 kW, 3.75 kW, and 4.52 kW, respectively. The existence of the γ-Al_2O_3 suggests that the deposited spray granules have reached melting state prior to impact on substrate. The higher plasma torch power provide a better heating due to on the one hand to a higher plasma flow enthalpy an on the other hand to a higher coefficient of thermal change and reduced material viscosity. This lead to a complete melting of the particles and their consequent rapid solidification [8, 15].

Yugeswaran et al. [8] indicated that the increase of the input power lead to the production of the aluminum oxide coatings with higher γ-Al_2O_3 phase content and decreases the average surface roughness values. Gao [10] also obtained that the amount of the γ-Al_2O_3 in the coatings increases with increasing plasma power. Meanwhile Zeng et al. [13] demonstrated that the smaller the size of starting powders was the better properties (microhardness, porosity) the coating possessed. Song et al. [15] also obtained that the increase of input power reduces volume fraction of α-Al_2O_3 phase and increases the hardness of the nanostructured aluminium oxide coatings.

The XRD results (Fig. 3) demonstrate that α-alumina and γ-alumina are found in the as-sprayed coatings. It may be noted that for higher torch power, the percentage of α-Al_2O_3 phase decreases and totally disappears at the highest input power. The reason for the difference in phase composition lies in the size of starting granules and input powers. The smaller granules (5 µm – 10 µm) will be melted faster that the big one (30 µm – 50 µm). Also the smaller granules can be easily accelerated and heated by the surrounding gas in the hot core of plasma [7]. Meanwhile the larger particles tend to penetrate the core and travel around the periphery of the plasma jet. Also the larger the granule size, the higher total heat capacity, thus it need more time or higher flow temperature to be melted. Hence the increase of torch power lead to the increase of the plasma flow temperature. As a result of this the melting degree of the particles increases and quantity of the fully melted granules becomes higher. Gao et al. [10] suggested that the undercooling of liquid droplets is such that γ-Al_2O_3 nucleates in preference to α-Al_2O_3, due to lower interfacial energy between the γ-Al_2O_3 structure and the liquid. Also

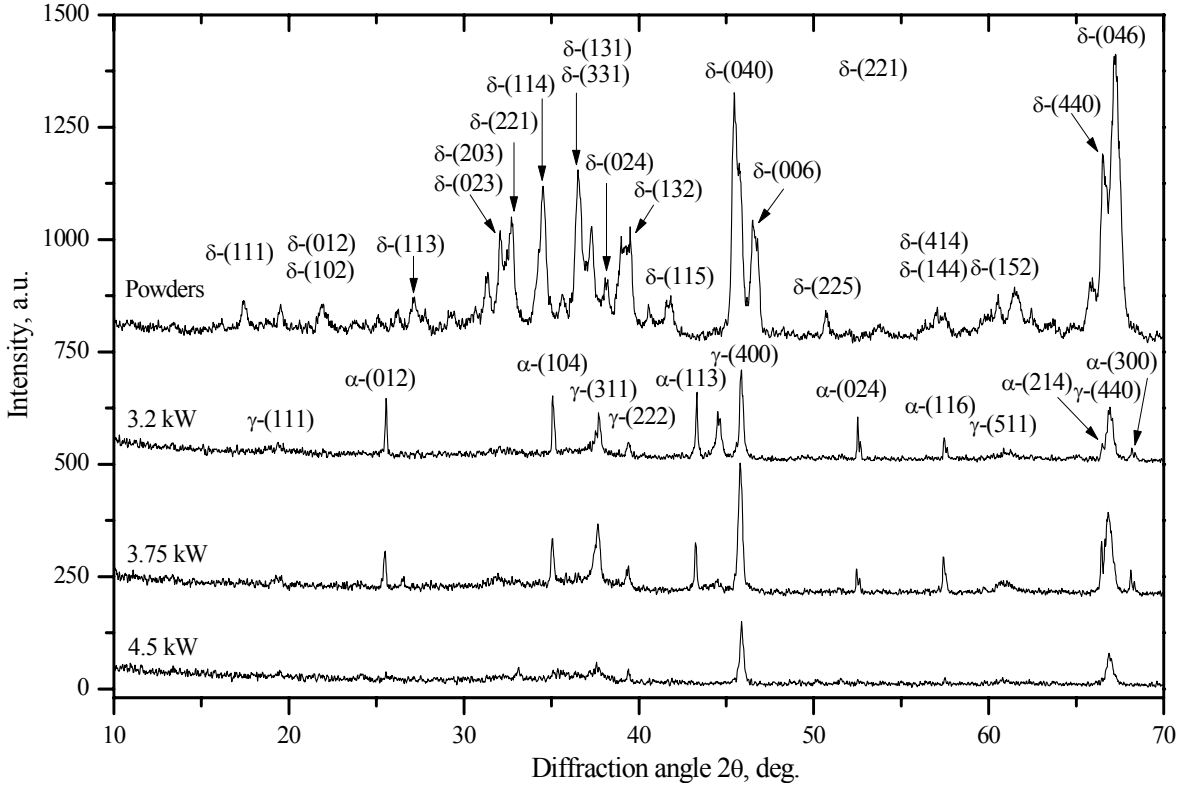

Fig. 3. XRD patterns of Al_2O_3 granules and coatings

the cooling rate after solidification is sufficiently rapid to prevent transformation γ-Al_2O_3 to α-Al_2O_3.

The crystalline size for γ-Al_2O_3 (400) crystallographic orientation was estimated according to Eq. (1) to be 97 nm (3.2 kW), 88 nm (3.75 kW), and 49 nm (4.52 kW). While the α-Al_2O_3 (113) phases crystallite size is 128 nm and 91 nm, for 3.2 kW and 3.75 kW, respectively. It may be noted that the alumina coatings deposited at a higher input powers are composed of the smaller size nanocrystallites. Chen et al. [24] proposed that the small grain size in the coatings should be the result of re-crystallization in the plasma spraying process. The sub-particles sized 2 nm – 5 nm would act as nuclei of re-crystallization and grow up to 20 nm – 50 nm in well-melted area. Probably the same effect may occur during the presented investigations.

CONCLUSIONS

The alumina coatings have been obtained using granulated Al_2O_3 nanopowders at the atmospheric pressure by plasma spraying. It was observed that the grain size and the surface roughness decreases with increase of the torch power. The XRD measurements showed that the phase compositions of produced coatings are different from the feedstock powders. The results indicated that the γ-Al_2O_3 phase amount in as-sprayed coatings increases from 56.52 % up to 100 % with the increase of torch power from 3.2 kW to 4.52 kW, respectively. The coating produced at the highest power value is composed from the smallest size nanocrystallites.

REFERENCES

1. **Masalski, J., Gluszeka, J., Zabrzeski, J., Nitsch, K., Cluszek, P.** Improvement in Corrosion Resistance of the 316L Stainless Steel by Means of Al_2O_3 Coatings Deposited by the Sol-gel Method *Thin Solid Films* 349 1999: pp. 186 – 190.
2. **Young, E. J., Mateeva, E., Moore, J. J., Mishra, B., Loch, M.** Low Pressure Plasma Spray Coatings *Thin Solid Films* 377 – 378 2000: pp. 788 – 792.
3. **Seo, J. G., Youn, M. H., Park, S., Jung, J. C., Kim, P., Chung, J. S., Song, I. K.** Hydrogen Production by Steam Reforming of Liquefied Natural Gas (LNG) over Nickel Catalysts Supported on Cationic Surfactant-templated Mesoporous Aluminas *Journal of Power Sources* 186 2009: pp. 178 – 184.
4. **Bushey, T. J., Dzombak, D. A.** Ferrocyanide Adsorption on Aluminum Oxides *Journal of Colloid Interface Science* 272 2004: pp. 46 – 51.
5. **Pranevičius, L. L., Valatkevičius, P., Valinčius, V., Montassier, C.** Catalytic Behavior of Plasma-sprayed Al-Al_2O_3 Coatings Doped with Metal Oxides *Surface and Coatings Technology* 125 2000: pp. 392 – 395.
6. **Irisawa, T., Matsumoto, H.** Thermal Shock Resistance and Adhesion Strength of Plasma-Sprayed Alumina Coating on Cast Iron *Thin Solid Films* 509 2006: pp. 141 – 144.
7. **Yin, Z., Tao, S., Zhou, X., Ding, C.** Particle In-Flight Behavior and its Influence on the Microstructure and Mechanical Properties of Plasma-Sprayed Al_2O_3 Coatings *Journal of the European Ceramic Society* 28 2008: pp. 1143 – 1148.
8. **Yugeswaran, S., Selvarajan, V., Seo, D., Ogawa, K.** Effect of Critical Plasma Spray Parameter on Properties of Hollow Cathode Plasma Sprayed Alumina Coatings *Surface and Coatings Technology* 203 2008: pp. 129 – 136.
9. **Ctibor, P., Bohac, P., Stranyanek, M., Ctvrtlik, R.** Structure and Mechanical Properties of Plasma Sprayed Coatings of Titania and Alumina *Journal of the European Ceramic Society* 26 2006: pp. 3509 – 3514.

10. **Gao, Y., Xu, X., Yan, Z., Xin, G.** High Hardness Alumina Coatings Prepared by Low Power Plasma Spraying *Surface and Coatings Technology* 154 2002: pp. 189 – 193.
11. **Fauchais, P., Vardelle, A., Denoirjean, A.** Reactive Thermal Plasmas: Ultrafine Particle Synthesis and Coatings Deposition *Surface and Coatings Technology* 97 1997: pp. 66 – 78.
12. **Shaw, L., Goberman, D., Ren, R., et al.** The Dependency of Microstructure and Properties of Nanostructured Coatings on Plasma Spray Conditions *Surface and Coatings Technology* 130 2000: pp. 1 – 8.
13. **Zeng, Y., Lee, S. W., Ding, C. X.** Plasma Spray Coatings in Different Nanosize Alumina *Materials Letters* 57 2002: pp. 495 – 501.
14. **Chen, H., Zeng, Y., Ding, C.** Microstructural Characterization of Plasma-Sprayed Nanostructured Zirconia Powders and Coatings *Journal of the European Ceramic Society* 23 2003: pp. 491 – 497.
15. **Song, E. U., Ahn, J., Lee, S., Kim, N. K.** Microstructure and Wear Resistance of Nanostructured Al_2O_3-8wt.% TiO_2 Coatings Plasma-Sprayed with Nanopowders *Surface and Coatings Technology* 201 2006: pp. 1309 – 1315.
16. **Lima, R. S., Marple, B. R.** From APS to HVOF Spraying of Conventional and Nanostructured Titania Feedstock Powders: A Study on the Enhancement of the Mechanical Properties *Surface and Coatings Technology* 200 2006: pp. 3428 – 3437.
17. **Gadow, R., Kern, F., Killinger, A.** Manufacturing Technologies for Nanocomposite Ceramic Structural Materials and Coatings *Materials Science and Engineering B* 148 2008: pp. 58 – 64.
18. **Pawlowski, L.** Finely Grained Nanometric and Submicrometric Coatings by Thermal Spraying: A Review *Surface and Coatings Technology* 202 2008: pp. 4318 – 4328.
19. **Toma, F. L., Berger, L. M., Naumann, T., Langner, S.** Microstructures of Nanostructured Ceramic Coatings Obtained by Suspension Thermal Spraying *Surface and Coatings Technology* 202 2008: pp. 4343 – 4348.
20. **Chen, D., Jordan, E. H., Gell, M.** Effect of Solution Concentration on Splat Formation and Coating Microstructure Using the Solution Precursor Plasma Spray Process *Surface and Coatings Technology* 202 2008: pp. 2132 – 2138.
21. **Marcinauskas, L., Valinčius, V., Valatkevičius, P., Grigonis, A.** Investigation of Single-Chamber Linear Plasma Torch Characteristics While Heating Monatomic and Diatomic Gases *Power Engineering* 1 2006: pp. 36 – 41 (in Lithuanian).
22. **Khor, K. A., Boey, F. Y. C., Zhao, X. L., Cao, L. H.** Aluminium Nitride by Plasma Spraying of an Al_2O_3-C-Sm_2O_3 System *Materials Science and Engineering* A 300 2001: pp. 203 – 210.
23. **Suresh, K., Selvarajan, V., Vijay, M.** Synthesis of Nanophase Alumina, and Spheroidization of Alumina Particles, and Phase Transition Studies Through DC Thermal Plasma Processing *Vacuum* 82 2008: pp. 814 – 820.
24. **Chen, H., Gou, G., Tu, M., Liu, Y.** Characteristics of Nano Particles and Their Effect on the Formation of Nanostructures in Air Plasma Spraying WC-17Co Coating *Surface and Coatings Technology* 203 2009: pp. 1785 – 1789.

DOI: 10.5755/j02.ms.26042